Heliyon 9 (2023) e19553

Contents lists available at ScienceDirect

Heliyon

journal homepage: www.cell.com/heliyon

A novel multipurpose device for dataset creation and on-device immediate estimation of blood glucose level from reflection ppg

Kazi Mosaddequr *, Tanzilur Rahman

Department of Electrical & Computer Engineering, North South University, Dhaka 1229, Bangladesh

A B S T R A C T

We propose a completely non-invasive and highly accurate portable blood glucose estimator, which is simple hardware that anyone, regardless of their prior experience or knowledge, can use to obtain an immediate reading of their blood sugar level. Glucose levels can be monitored in real time and displayed on the device thanks to its infrared LED light source, sensor with built-in amplification unit, processing unit with blood glucose regression model, power management unit for autonomous operation, and display. The device was initially used to create a dataset of photoplethysmography (PPG) signals collected from the fingertip of 50 subjects. The extracted signal features were correlated with the subject's glucose level, which was measured at the same time using a commercial glucometer, and several regression models were constructed. The models were evaluated using signals from up to 110 subjects across three datasets, and the most optimized model was implemented in the device to predict the subject's blood glucose level solely based on PPG in real-time. The device with the built-in model has been subjected to extensive testing to gauge its efficacy. The device's clinical accuracy is encouraging. The pricey strips and needles that must be purchased along with the hardware in the conventional method will no longer be necessary with this device.

1. Introduction

Diabetes is one of the most severe and common chronic diseases. It shortens life expectancy and causes costly, incapacitating, and life-threatening complications. According to the International Diabetes Federation (IDF) report, there were 463 million adults who had diabetes during the pandemic as of 2019 [1]. The aging of the population, obesity, and other factors are to blame for the rise in diabetes. As a result, it's important to monitor blood sugar levels. To measure blood sugar levels, numerous methods have been developed [2]. However, no significant progress has been made in improving the painful method of measuring blood sugar levels in the last 25 years [3]. Although the conventional invasive method is highly accurate, it has several drawbacks, including being expensive, painful, and risky.

Many approaches [4] have been taken to solve these problems, including the minimally invasive method [5–7], the non-invasive fluid sampling method [8–10], and the non-invasive optical method [11] to inform users of their glucose levels. Some works argue about the equilibrium of blood glucose levels corresponding to vitreous eye fluid [12] and saliva [13,14].Non-invasive optical approaches have recently gained popularity [15,16,17]. [15] proposed a PPG device that can monitor hemoglobin, glucose, and creatinine. They compute glucose levels and other vital factors using a genetic algorithm and Fourier analysis [16]. proposed a similar study that uses PPG signals to extract physiological health data and plans to build a commercial prototype of the PPG system [17]. proposed a novel technique, such as a microwave-based detection strategy, to improve the detection resolution of blood glucose levels.

However, the majority of these methods are still in the modeling and simulation stages and have yet to be implemented in standalone prototypes. Some lack accuracy and reproducibility, both of which are critical for medical devices. If a patient desires high

* Corresponding author.
E-mail addresses: kazi.mosaddequr@northsouth.edu (K. Mosaddequr), tanzilur.rahman@northsouth.edu (T. Rahman).

https://doi.org/10.1016/j.heliyon.2023.e19553
Received 4 January 2023; Received in revised form 1 April 2023; Accepted 25 August 2023
Available online 1 September 2023

accuracy, he or she must use a traditional invasive method, which opens the door to future complications such as infection. However, if a patient uses non-invasive fluid or optics, the device's accuracy suffers. In the last ten years, advances in data science and machine learning have helped people understand the inherent property of data, which can be used to relate with other variables and produce desired results. Similarly, advances in semiconductor technologies mean that low-cost, miniature devices are now possible. As a result, many portable ready-made medical devices are now on the market. Advances in data science and semiconductor technology give us hope of creating something better and less painful.

In this paper, we propose a low-cost, painless Blood glucose level detector that requires little skill and knowledge to operate. This multipurpose device can be used to generate a ppg dataset, build a model, or even function as a standalone non-invasive glucometer. This device collects reflection ppg data from the subject's fingertip using a dedicated sensor (OPT101) and light source (infrared LED light). To connect the device to the PC during data collection, a graphical user interface (GUI) program has also been developed. This program includes features for visualizing the quality of the acquired signal in real-time during data collection, saving it to the cloud, associating the actual label with the signal, and creating a good-quality dataset automatically. Before extracting various features from the acquired signals, they are cleaned. For the quantitative analysis of glucose levels, various Principal Component Regression models were built using the extracted features. To gain additional insights, the models were trained and tested on a larger dataset containing up to 110 subjects collected previously by the same group using different methods for the same purpose (smartphone ppg). The optimized model has been loaded into the device's processor, allowing the user to predict glucose levels in real time and instantly. The integrated model device was tested on a user for seven days, and performance was assessed by comparing actual glucose levels. The results show that the accuracy is clinically significant.

This work's significant contribution is thus:

- A non-invasive glucometer that is very small, low-cost, and portable (3x3) has been proposed.
- The proposed device predicts glucose levels in less than 2 min.
- The device's accuracy is very high (0.7850 mmol/L), which is comparable to the literature.
- In addition, a hardware and software platform for generating high-quality datasets is proposed.
- In addition, a fully personalized model for future implementations is demonstrated.

2. Background

M. R. Haque et al. [15] proposed to measure hemoglobin, glucose, and creatinine using PPG signal collected from smartphone video. Using genetic algorithms and Fourier analysis, 46 features were extracted from the PPG signal. A DNN volume-based model with ten-fold cross-validation was used. Though red and infrared LEDs are best for measuring blood sugar levels, they used green light, which scatters significantly more than red and infrared light. They used two machine learning algorithms, and the DNN model's final proposed best-estimated accuracy is $R2 = 0.902$ for Gl (Glucose level). In contrast, we propose a fully standalone hardware prototype capable of detecting glucose levels in real-time with greater accuracy. Our device can process data within the hardware and return a result in a matter of minutes.

Gupta et al. [16] propose using PPG signals to extract physiological health parameters, with the goal of developing a commercial PPG system prototype. They used the XGBooster regression algorithm and a Random regressor model decision tree-based method. The proposed algorithm and system have clinical accuracy in predicting BGL levels. Their work is illuminated by green, red, and infrared leds. The device cost may rise in comparison to ours due to additional circuitry used to clean the PPG signal received from the green light.

Islam et al. [18] proposed smartphone-based detection, which included the acquisition of a brief video. After that, the video was split into frames, and data from the red channel was used to generate a Photoplethysmography (PPG) signal. A Gaussian filter and the Asymmetric Least Square (ALS) method were used to remove high-frequency noise and motion interference from raw PPG signals, which are common in such signals. The glucose levels were predicted using the Principal Component Regression (PCR), Partial Least Square Regression (PLS), Support Vector Regression (SVR), and Random Forest Regression (RFR) models. PLS with an unbiased dataset had the lowest standard prediction error (SEP) at 17.02 mg/dL, according to their experiment.

Golap et al. [19] proposed a non-invasive hemoglobin and glucose level estimation model based on multigene genetic programming (MGGP) and photoplethysmograph (PPG) characteristic features extracted from smartphone fingertip video. A finger was sandwiched between the smartphone camera and the Near Infrared (NIR) board to capture the video. Finally, using a feature set based on PPG signal and user information, an MGGP-based symbolic regression model was developed to estimate hemoglobin and glucose levels. The best results (0.304 for hemoglobin and 0.324 for glucose) are obtained using selected features and symbolic regression based on MGGP. This type of device is dependent on the smartphone, camera sensor quality, and additional circuitry. In comparison to our simpler and lower cost portable on chip solution, the device itself can be quite bulky and expensive.

In contrast to the NIR sensor proposed in our work, Omer et al. [20] presented a portable planar microwave level sensor for fast, accurate, and non-invasive monitoring of blood glucose levels as an effective method for diabetes control and prevention. Four hexagonal cells of split ring complementary resonator (CSRR) are arranged in a honeycomb cell configuration and are fabricated on a thin sheet of FR4 dielectric substrate. The improved design of the CSRR sensing element, which exposes glucose samples to intense interactions with highly concentrated electromagnetic fields around the sensing region, is credited with the high detection efficiency achieved in this work. This capability enables the developed sensor to detect subtle changes in the electromagnetic properties of glucose samples at various levels.

Li et al. [17] propose using microwave detection techniques to improve the resolution of detected blood glucose levels. To extract

the poles of received microwave signals, the matrix pencil method is used. By training the poles extracted from the received signals, the artificial neural network can help distinguish the blood glucose level. The reported mean error between the actual blood glucose level and the detected blood glucose level can be very small. The UWB microwave detection system can detect plasma glucose levels in the normal range of 70–240 mg/dl.

Muller et al. [21] propose impedance spectroscopy as a non-invasive continuous glucose monitoring method in humans. The impedance spectra were summarized using principal component analysis, and the relevant variables were identified using Akaike's information criterion. In the impedance spectra, the principal component analysis identified two immediate impacts: a blood glucose-related process and an equilibration process related to skin and underlying tissue moisturization. However, other factors, in addition to glucose, have a significant influence on the impedance properties of the skin and the tissue beneath it, making this approach less reliable.

The current study's authors previously presented work [18] on non-invasive glucose level measurement with smartphone sensors. The difference between that work and the current effort is that it was proposed primarily for simulation and model development, whereas the current effort developed a data-gathering tool and a fully functional prototype. Furthermore, our current prototype is a dedicated independent low-cost hardware design, whereas previous work was reliant on expensive smartphones with high-quality sensors. Previous research was conducted in a controlled environment, and no data variance or classification was obtained. In contrast, for data variation and bias reduction, we divided subjects into gender and age groups. We believe that the most significant benefit of this work is improved accuracy and outcomes, which are the result of cleaner signals.

3. Methodology

Initially, a sensor-equipped device was used to collect data (PPG signal) from subjects. The collected data was then used to develop a model. The model was then loaded into the device and tested in real time. The research protocol was approved by the NSU Institutional Review Board/Ethical Review Committee (IRB/ERC). In addition, all subjects involved in the study provided informed consent. The entire procedure, as shown in the top part of Fig. 1, is non-invasive, in contrast to the existing traditional invasive technique, which is also shown in Fig. 1.

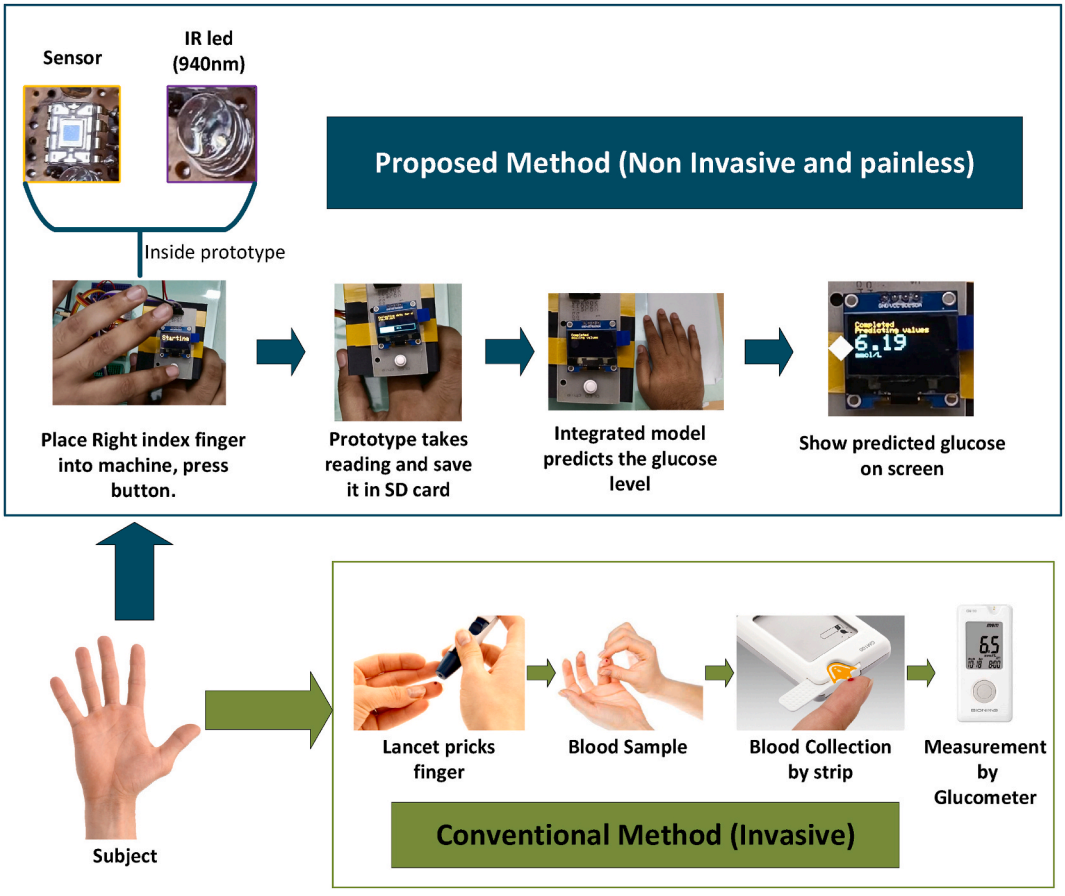

Fig. 1. System diagram of our proposed device.

3.1. Hardware design

The proposed hardware contains a sensor, a processor, a display, and a storage unit. The details on each unit are provided below:

3.1.1. Sensor unit

The Sensor unit's purpose is to collect the PPG signal from the fingertip. The sensor unit is made up of an OPT101 chip, a capacitor, an infrared LED, and a resistor. Fig. 2(a) depicts how the component should be connected. The capacitor is required for the operational amplifier in OPT101 to smooth out the PPG signal. It also eliminates the zero-correction error in the data received. To protect the resistor, it is linked to an infrared LED. This PCB is linked to other PCBs, such as the CPU unit, via a SILO connector. The OPT101 is a monolithic photodiode with an on-chip impedance amplifier. Combining a photodiode and an obstacle amplifier on a single chip eliminates problems associated with separate devices, such as leakage current errors, noise capture, and capacitance spikes. The output voltage is proportional to the amount of light emitted. As a result, the amplifier can operate in either single or dual mode. The internal diagram of the OPT101 is available in the datasheet [22]. For infrared light emission, we used a 5 mm IR LED with a wavelength of 940 nm. This wavelength was chosen because it can penetrate the skin and tissues and be absorbed by the glucose molecule. Additionally, we experimented with 5 mm red and 5 mm white LEDs. These two LEDs, however, introduce noise into the voltage peak reading. Furthermore, the white LED requires 5V to fully illuminate our finger, which is a disadvantage given the processor's voltage reading of

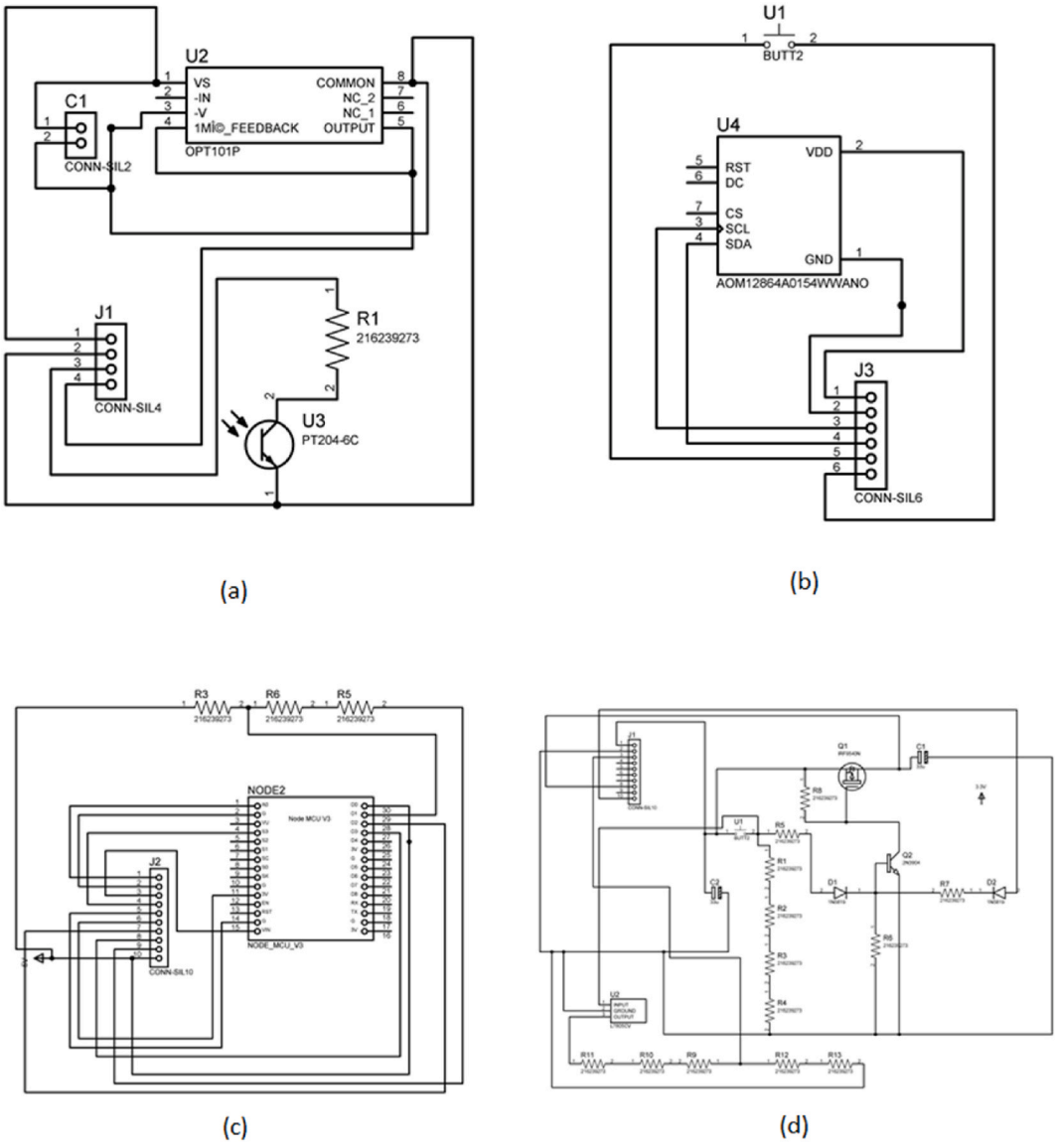

Fig. 2. All schematic diagrams of the circuits developed; (a)Sensor Unit, (b)Display unit, (c)Processor unit, and (d) Power latch for one-click power.

3.3V.

3.1.2. Processor unit

The processor unit is used to process and calculate the predicted result. The processor unit has only the ESP32 chip, as shown in Fig. 2(c). The resistors present on the processor chip come from the latch unit. Installing the resistors in the latch unit was difficult because of the size increase. Consequently, it was placed within the power unit to reduce the size of the latch circuit. ESP32 has been utilized for data collection and processing. Designed by Espressif Systems, the ESP32 is a low-power system chip (SoC) with dual-mode Wi-Fi and Bluetooth connectivity. The ESP32 includes a built-in antenna switch, RF balun, power amplifier, low-noise receiving amplifier, filter, and power management module. The ESP32 achieves extremely low power consumption by utilizing power-saving technologies like high clock sync resolution, various operating mode power supplies, and dynamic capacity expansion. This CPU was chosen above other popular processors like the Arduino atmega328p due to its low power consumption and compact size. Low power usage offers the added benefit of increasing the battery's life. In addition, the latch was created to activate/deactivate the circuit with a single button and thus conserve energy. It is also programmed to shut down automatically after a predetermined period of inactivity; therefore, the user is not always required to turn off the circuit manually.

3.1.3. Display unit

The output needs a display for the user's convenience because we sought to create a fully portable glucose monitoring device. The display unit includes a 0.99-inch OLED display, a button, and a SILO connection, as shown in Fig. 2(b). The predicted glucose value and message are displayed on display. The advantages of an OLED display include its thinness, portability, and low power consumption. Backlighting doesn't require a different voltage, in contrast to LCDs. In order to save energy, small LEDs can also be turned off when not in use. The I2C connection capability of ESP32 makes it easy to integrate the processor's display. SILO connects the button to the latch and processing unit. Additionally, the button serves as a universal button to improve accessibility.

3.1.4. Latch unit

A latch unit is created to increase the accessibility of the device by terminating unwanted buttons. As depicted in Fig. 2(d), the latch unit consists of a capacitor, inverter, transistors, voltage regulator, and resistors. It can power down the machine when it detects inactivity. The ESP32 transmits a signal to the latch unit to power down the device. Consequently, it eliminates the necessity for a complicated power button. In addition, it regulates the battery's excessive voltage to prevent accidents, as ESP32 operates on 3.3V.

3.1.5. Storage

The PPG signal collected from the user must be stored temporarily in the device before further processing. ESP32 has SRAM called RTC fast memory. However, the reliability of this memory depletes with high usage. Due to the fact that the proposed device must store approximately 1500 data points each time a user uses it and during data processing, the device's dependability may decrease over time. Therefore, an SD card module, a 32 GB micro SD card, has been used to solve memory issues. The micro SD card needed to be

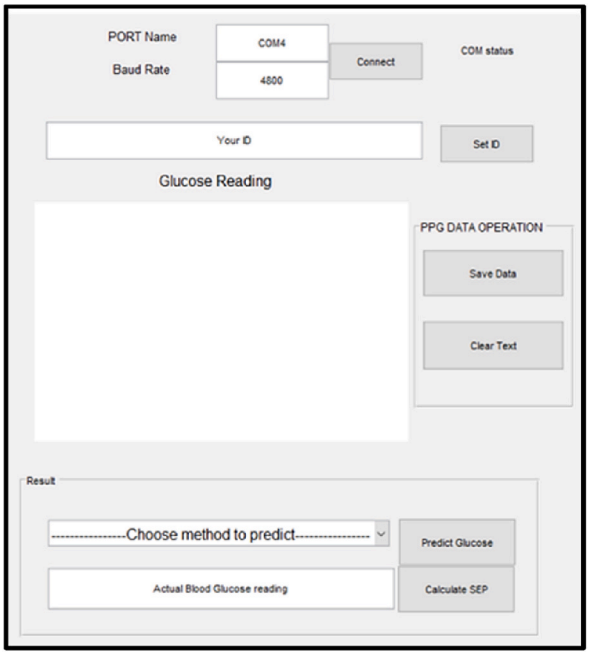

Fig. 3. Graphical User Interface for data collection.

formatted in the FAT32 system, and some directories had to be made before it could be used for our prototype. WEMOS SD card shield was used for interfacing. It supports both 3.3V and 5V voltage input.

3.2. Data acquisition

This section describes how data were collected noninvasively with the proposed device and invasively with a clinical device. In addition, we will also discuss how research participants were selected and informed.

3.2.1. Acquisition software

As shown in Fig. 3, a graphical user interface (GUI) program was developed to facilitate data collection. The software is straightforward, user-friendly, and equipped with several features that facilitate data collection. First, a USB cable must connect the hardware to the workstation (a laptop in our case). Before beginning the experiment, the invigilators were required to enter the port name, baud rate, and click connect button. This enabled researchers to experiment with a variety of devices and baud rates. The software connects the device to the workstation when the connect button is clicked. A user ID, located in the header of the consent form, was required. Moreover, ID numbers are unique and never duplicated. When the user is ready to provide data, a physical button on the hardware is pressed to initiate the data collection process. Each file obtained in this format has the name 1234_5, where 1234 is the id number and 5 represents the fifth trial. A code is executed in the background to determine if the directory contains a file with the specified ID. If the file already exists, it will look for the sub-part of the file name that contains the previous trial number and increment it to create a new file name. Once the file has been created, a graph displaying the PPG signal in real-time will appear in a separate window. While the graph is displayed, PPG points are recorded in the resulting file. When the data collection is finished, the graph window is closed. If the real-time graph is satisfactory, the user clicks the save button to store the PPG data. The investigator is permitted to repeat the investigation as frequently as desired. To maintain the security and accessibility of our data, the Google Drive desktop client synchronized the folder where records are saved in real-time. Fig. 4 is a summary of the entire procedure.

3.2.2. Acquisition of PPG signal

We chose 50 subjects from three age groups to collect PPG signals with the proposed hardware (10–20 years, 21–40 years, and 41+ years). Section 3.4.1 details the distribution. Subjects were instructed to sit in their assigned seat in order to be comfortable and obtain stable readings. The invigilator set a unique ID in the Graphical User Interface (GUI), and connected the device to the laptop while the subject was resting. The subject was then instructed to place their left index finger on the device's sensor unit. The invigilator clicks the button after successful placement, and the PPG reading appears on the Laptop screen. If the invigilator believes the data is acceptable, it is saved. The procedure is repeated three times until three good readings are saved. Following the non-invasive portion, the invigilator cleans the right index finger and measures blood glucose with a commercially available glucometer (Bionime GS100). The informed consent form was signed by all of the subjects. During the data collection, proper hygiene was maintained.

Allowing the subject to relax for a few minutes before placing their fingertip on the sensor was found to be the most effective method for obtaining PPG data with minimal mobility [18]. Fewer motion interferences are introduced because they remain quiet and still. During data collection, other methods that prompted participants to move their finger frequently were also modified. Distortion can cause dispersed plots, and captured signals can have significant baseline variations. Data acquisition using our recommended device is more precise than video data acquisition, as stated in section 4.1. Refer to our previous work [18] that contains more information on PPG signals, signal cleaning, processing and analysis.

3.2.3. Acquisition of glucose level

The subject's actual blood sugar levels were obtained invasively as a reference during the investigation using a commercially available medical standard glucometer. A little droplet (1–2 μL) of blood obtained from the subject's fingertip can measure the

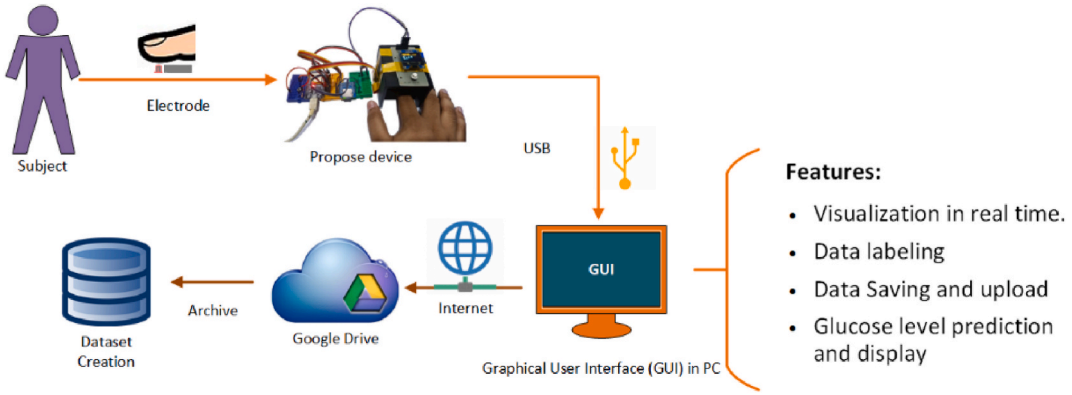

Fig. 4. Feature of GUI

subject's blood sugar level. It is effective between 10 and 600 mg/dL. In addition to the meter, this method requires a single-use test strip and single-use safety lancets. First, the subject's hand was cleansed with a hand sanitizer and alcohol solution before the blood sample was obtained. Then, a test strip was inserted into the glucometer to prepare it for glucose measurement. Next, using a lancet, blood was obtained by pricking the side of any finger. The punctured finger was then contacted and held against the test strip's edge to transfer the blood drop from the finger to the test strip. Finally, a band-aid was applied to the punctured finger. The glucometer typically processes samples in 5–8 s and displays the glucose concentration in mg/dL on the screen. Each individual had at least one trial collector to determine the reference value.

3.3. Model building

The collected PPG signals and their reference (actual glucose level) were compiled into a single file to create a dataset. Data scaling was then performed on the PPG signals to eliminate the variations of voltage levels and represented between 0 and 1. The data set was divided into an 80:20 train test ratio. To generate models, the data was fed into Principal Component Regression (PCR), a statistical learning algorithm. Several filters, including Asymmetric Least Square (ALS) and the Gaussian filter, were implemented during the construction of the model, and several features, including time difference between peaks, characteristic points, first derivative of characteristic points, and second derivative of characteristic points, were extracted and combined with PCR. The predicted value of the model was then plotted in a Clarke Error Grid. Finally, the model with the lowest SEP was chosen for deployment in real-time testing hardware.

Fig. 5 depicts an overview of software models developed for non-invasive blood glucose determination.

3.3.1. Dataset

Fig. 6 shows the distribution of 50 people chosen from three age groups (10–20 years, 21–40 years, and 41+ years) for data collection. The age group was chosen to add diversity to the data collected and to help build a generic model. The participants were fully informed of the procedure before collecting their PPG signals. Then, each person went through trials until at least three optimal PPG signals were obtained. Each recorded signal has 60 s of data. However, 5 s were initially removed from the segment's beginning and end. This was done due to the natural prevalence of significant motion artifacts in the beginning and end of a recording. As a result, this experiment produced a 50 s PPG signal per trial per subject. During the collection of reference values, a commercially available glucometer (Accu-Check Active) with DIN EN ISO 15197:2 accuracy was used. All participants signed a consent form and kept themselves clean. Before taking PPG readings, the subject's fingers and sensor lenses were cleaned with alcohol wipes. The obtained data are then transformed using the Min Max Scaler to produce data with identical ranges.

3.4. Features

Several features have been extracted from the PPG signals collected as part of the data from users. These include systolic peaks, diastolic peaks, the time difference between systolic and diastolic peaks, the signal's first derivative, the signal's second derivative, and peaks that appear in the signal's first and second derivatives.

3.4.1. Systolic and diastolic features

The systolic peak is the direct pressure wave traveling from the left ventricle to the body's periphery. Conversely, the pressure wave

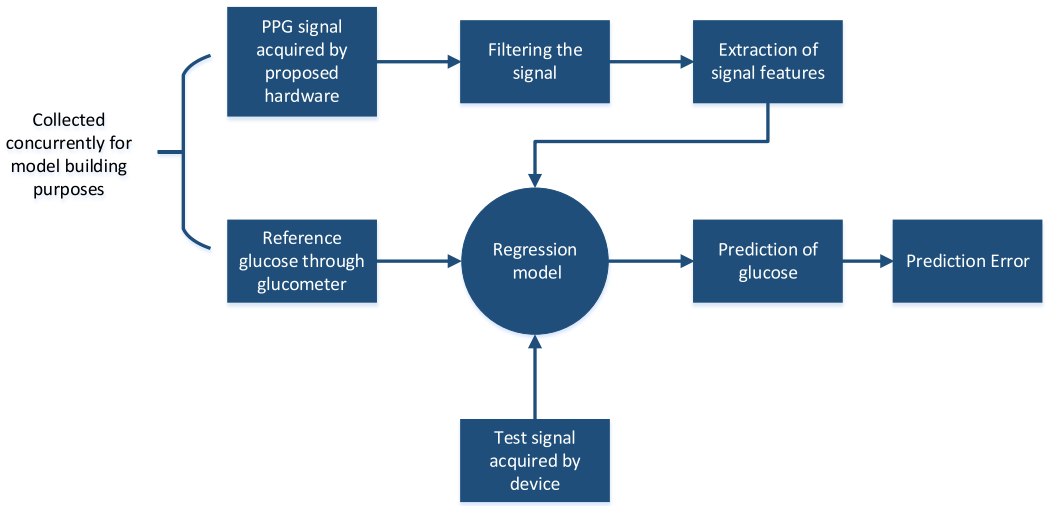

Fig. 5. Flowchart describing the suggested method for the non-invasive determination of blood glucose level utilizing a sensor.

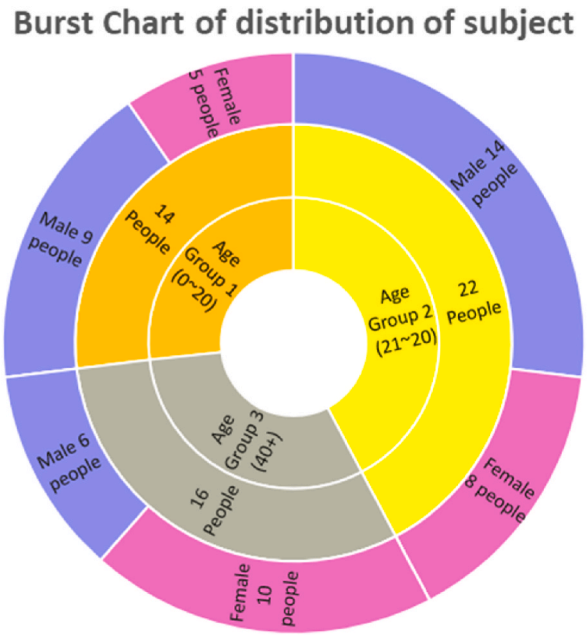

Fig. 6. Chart showing the distribution of age groups in the experiment.

reflections by the lower body's arteries constitute the diastolic peak. Fig. 7 (a) demonstrates that each cycle of the PPG signal consists of a systolic and diastolic peak. These peak positions were retrieved from the PPG signal as features.

DelT denotes the period between the systolic and diastolic maxima. It was calculated using each pair of systolic-diastolic signal peaks. Using the time difference between the systolic and diastolic peaks in each cycle of the preprocessed PPG signal, DelT values were saved in an array. In Fig. 7(a), a representative PPG signal displays systolic, diastolic, and DelT characteristics.

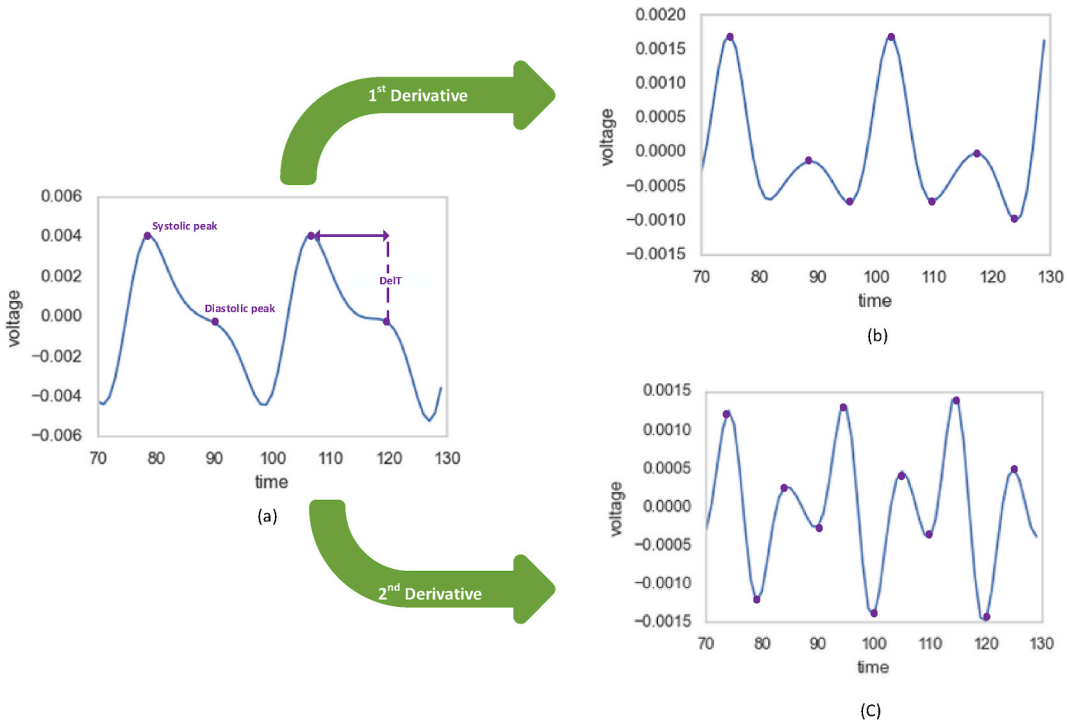

Fig. 7. (a) is a representative PPG single-cycle waveform with systolic and diastolic peaks and DelT; (b) is the first derivative of that cycle, and (c) is the second derivative of the cycle.

3.4.2. First derivative features

Typically, the first derivative represents the instantaneous rate of change. It displays whether the function is rising or decreasing its rate of increase or decrease. Since PPG is a periodic function, the number of peaks (features) inside the PPG signal increased following the first derivative. Therefore, a two-point central difference approach was utilized for determining the PPG signal's first derivative, as illustrated in Equation (1).

$$d(j) = \frac{1}{2}(a(j+1) - a(j-1)) \tag{1}$$

a(j) is retrieved from the existing preprocessed array, whereas d(j) is put in a new array. Since the first derivative signals also included negative peaks, the signal was further processed before extracting the derivative signal's attributes. This makes the signal more apparent, allowing for easy extraction of its features. Fig. 7(b) depicts a derivation of an example PPG signal, with the extracted features highlighted.

3.4.3. Second derivative features

Similar to the first derivative, the second derivative is a derivative of the slope. Additionally, it raised the signal's peaks (features) that exceed the first derivative. Equation (2) shows that the second derivative was computed using a three-point central difference approach.

$$d(j) = a(j+1) - 2a(j) + a(j-1) \tag{2}$$

a(j) represents the points in the existing preprocessed array, while d is the array's newly calculated second derivative. Fig. 7(c) depicts the second derivative of a sample PPG signal, with the extracted characteristics also indicated. The illustration illustrates how the first and second derivatives boost the peaks of a PPG signal.

3.5. Principal Component Regression (PCR)

A regression analysis known as Principal Component Regression (PCR) was performed on the PPG signals and their references to estimate glucose concentration (collected by a clinical device). Various PCR-based models were built on raw signals, preprocessed signals, and features extracted from preprocessed signals to test and compare the efficacy of non-invasive quantitative estimates. PCR has been widely used in chemometrics as a multivariate calibration method, and these methods can be used when a dataset contains associated predictor variables. By linearly combining the previous predictor variables, this regression technique generates new predictor variables (components). Furthermore, PCR produces components regardless of the response values. As a result, the predicted

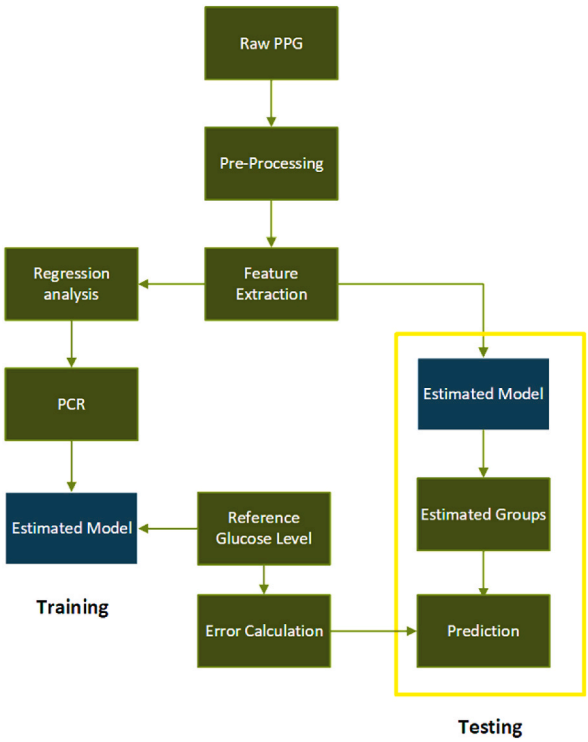

Fig. 8. Diagram showing the process of PCR in the experiment Taken from [18].

accuracy of this regression method is reliable. PCR was chosen for this study due to its reported high accuracy in predicting glucose concentrations from NIR (Near-Infrared) spectra. The detail diagram of PCR model is provided in Fig. 8.

Before building PCR models, the data was split at 80:20 between train and test data. Numerous feature extraction approaches were discussed in the preceding section. Models are created for each of the features that are used. The Clarke Error Grid was plotted to determine the model's validity, and SEP was calculated. For integration into the proposed device for real-time glucose level prediction, the model with the smallest SEP was chosen. The proposed device, which was integrated with the best PCR model, was tested for two weeks on a subject that will be discussed later.

3.6. Models generated by PCR

Various PCR-based models were built on raw signals, preprocessed signals, and features extracted from preprocessed signals. This section briefly overviews the eight PCR models, namely *Xraw, XrawALS, XrawALSGauss, XrawALSGaussDelT, XrawAlsGaussDeriv1, XDeriv1CharPoints, XrawAlsGaussDeriv2, XDeriv2CharPoints* developed by various techniques.

The PCR model based on the raw PPG signal obtained directly from the subjects was named X raw. This model was created as a baseline for the comparison of performance with other models. In the model *XrawAls*, the raw PPG signal was first filtered by Asymmetric Least Square (ALS) filter before feeding into PCR. ALS is an effective baseline correction method [23]. To eliminate motion interferences, ALS, which is useful for correcting data with relatively narrow peaks, was used. Furthermore, ALS facilitates the enhancement of the systolic and diastolic peaks, which are necessary for feature extraction. The overall signal quality was improved by lowering peak-to-peak variations as a result of ALS baseline correction.

Prior to using the regression method in the case of XrawAlsGauss, the signal was smoothed using a Gaussian filter to remove high-frequency noise. A preprocessing approach with ALS as the first stage and a Gaussian filter as the second stage considerably enhances the quality of the PPG signals collected. The Gaussian filter [24] is a nonuniform lowpass filter and is a common choice among general-purpose filters for removing the high-frequency components of a PPG signal. When tuned with the mean center frequency and standard deviation, this filter performs exceptionally well as a bandpass filter in the frequency domain. The gaussian filter can be explained by Equation (3):

$$G(x) = e^{\frac{(x-c)^2}{2\omega^2}} \tag{3}$$

Here, the standard deviation can be modified by adjusting the degree of smoothing. For example, when the center frequency was adjusted to c = 0.068 and the standard deviation was set to w = 0.0543, it functioned optimally in smoothing the PPG signal.

In the *XrawAlsGaussDelT* model, the raw PPG signal was processed through ALS and Gaussian filter to eliminate high-frequency noise. Then systolic and diastolic peaks are identified, and their time differences are noted. These features are then applied to regression analysis to generate a model. DelT denotes the period between the systolic and diastolic maxima. It was calculated using each pair of systolic-diastolic signal peaks. Using the time difference between the systolic and diastolic peaks in each cycle of the preprocessed PPG signal, DelT values were saved in an array. In Fig. 7(a), a representative PPG signal displays systolic, diastolic, and DelT characteristics.

In *XrawAlsGaussDeriv1* and *XrawAlsGaussDeriv2*, the raw PPG signal was preprocessed like before. 1st derivative and 2nd derivative were then computed on the preprocessed signal before feeding into PCR to generate respective models.

All of the steps in the XDeriv1CharPoints model are the same as in the XrawAlsGaussDeriv1. However, the peaks of the signals were detected after calculating the first derivative. These are also known as 1st derivative characteristics points. Based on these characteristic points, the PCR model is built. All of the steps are the same as for XDeriv2CharPoints and XrawAlsGaussDeriv2. The peaks of the signals have been detected after calculating the 2nd derivative, which are also known as the 2nd derivative characteristics points. These characteristic points are used to generate the PCR model. Fig. 7(b) and (c) show the first and second derivative characteristics points.

3.7. Integration of the model in hardware

We chose one of the eight models with the lowest SEP to use in the proposed device's processing unit for real-time glucose level estimation. As a result, the following equation was used to estimate the glucose level within the device:

$$y_P = y_M + (((X_D - X_M) * P) * C)$$

where,

y_P is the predicted y value, the predicted glucose in our case.

y_M is the mean y value generated by the model used.

X_D is the x value of PPG from the user.

X_M is the Mean of all the x values of PPG from the user.

P is the Principle value obtained from the model.

C is the component values obtained from the model.

Here, the values y_M, P, and C are extracted from the most optimized model, one of the eight models with the lowest SEP, and saved in a data file on device memory. On the other hand, X_D and X_M come from the data collected from the user on the test. For this, we

first collect data from users and store it in a directory. While collecting data, we also store the highest, lowest, and (highest - lowest) data readings. Then Mean Max scaling is applied to the data and stored in another directory along with the Mean of all x points.

Now that the model's hardware is self-sufficient in performing the estimation task, a user must place a finger on the sensor and press the button to begin taking the reading. When the reading is complete, an alert will appear on the OLED display to remove the finger. The processor will then perform the necessary calculations and display the predicted reading. The entire process has a Graphical User Interface displayed on the screen for the user's convenience. Even while waiting or processing, a progress bar will appear to show how much processing or data collection has been completed and how much remains. The entire procedure takes about 2 min, including data collection and glucose estimation.

4. Result

4.1. Hardware implementation

The entire hardware has been designed and implemented to be as small as possible in order to maximize portability and patient comfort. Fig. 9 depicts the device with various hardware units visible. A small enclosure has been constructed to block out any external lights that may interfere with signal acquisition. Fig. 10 shows that the proposed device outperforms smartphone-based methods previously used in the literature in acquiring PPG signals. When acquired with the proposed device, the PPG signal is sharper and cleaner, both the systolic and diastolic peaks are visible, and no baseline variations are present (Fig. 10 a). Consequently, there is no need for a baseline correction algorithm. Thus, the processing power and resources necessary to implement the algorithm are conserved. In contrast, the systolic and diastolic peaks of the PPG signal recorded by the mobile device are frequently obliterated (Fig. 10 b).

4.2. Data distribution

We used a variety of graphing techniques to determine the distribution of the data we collected. In addition, we attempted to visualize numerous aspects of the collected data. The Kernel Density Estimate (KDE) Plot, for instance, is used to visualize the Probability Density of a continuous variable. It depicts the probability density at different values of a continuous variable. In addition, we can print a single graph for multiple samples, allowing for a more efficient data representation. Fig. 11's KDE depicts the distribution of glucose levels among the participants in our experiment. The majority of glucose levels measured were around 5 mmol/L. However, significant data has also been collected on diabetics, as the smaller bubble above the larger bubble indicates.

A scatter plot is a graph that plots the values of two variables along two axes. In addition, the accompanying diagram depicts the frequency of respondents' glucose levels based on their gender and age. Given that the graph in Fig. 12 is spread, we may assume that the collected data is distributed evenly.

4.3. Experiment with models

Several PCR models were developed using various PPG-extractable characteristics. The sections that follow describe the observed outcomes of the various regression techniques used to predict blood glucose levels and compare the shown methods.

First, we divided the dataset in a ratio of 80%–20%, and then we constructed multiple models for training and testing. This step is

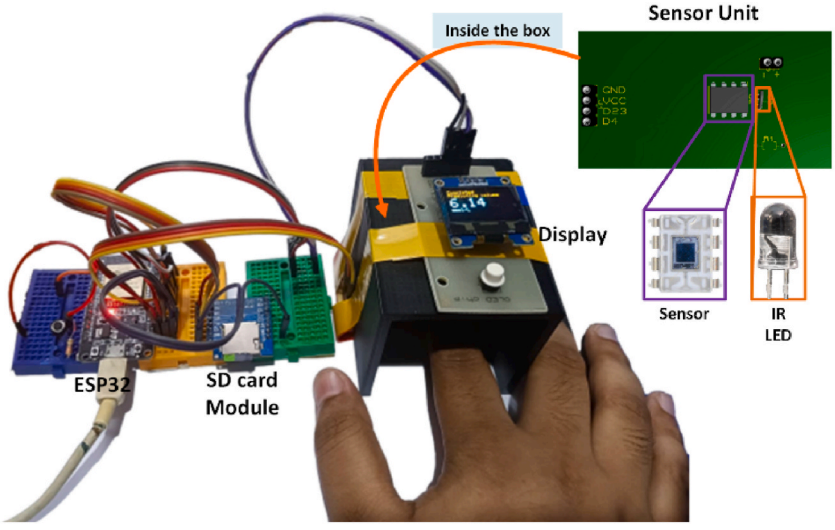

Fig. 9. Prototype of the final standalone circuit.

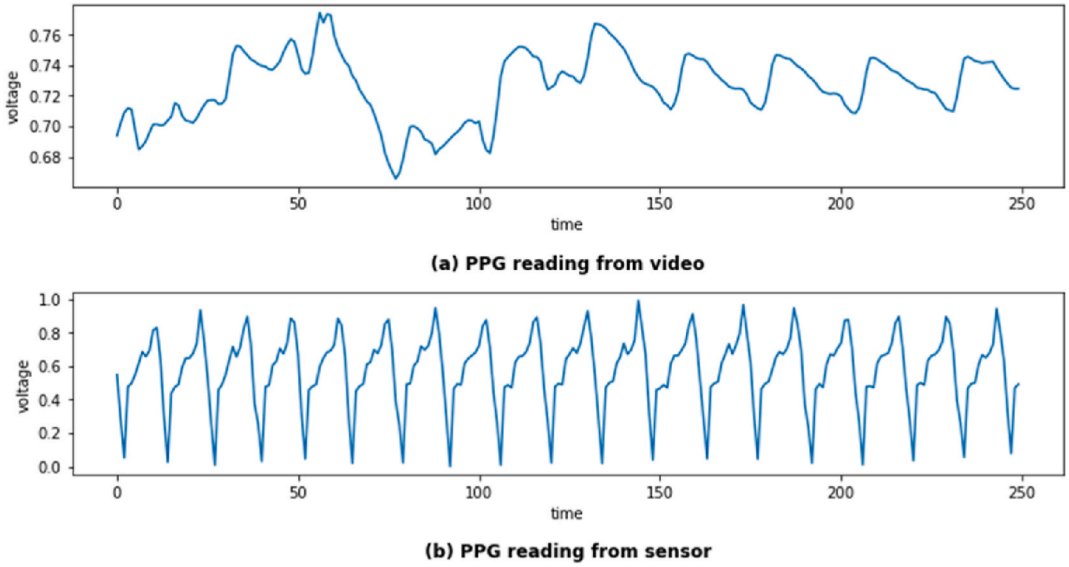

Fig. 10. Difference in obtained data; (a)PPG reading from video, (b) PPG reading from the sensor of our proposed device.

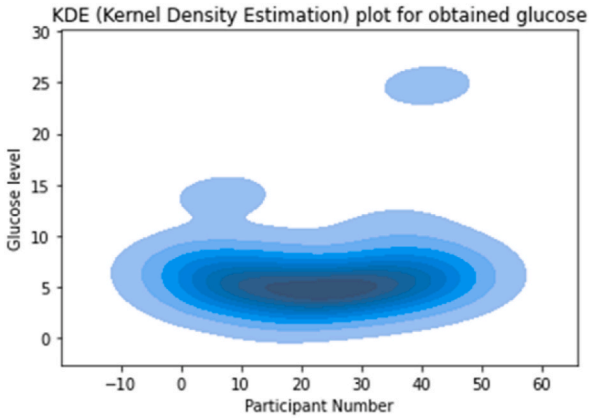

Fig. 11. KDE of the obtained data.

performed on a computer to identify the optimized model. The model that achieved high accuracy was then incorporated into the proposed hardware and evaluated in real time using subject-specific, completely unbiased test cases. Additionally, model building is performed on both single and merged datasets. The experimental results performed on the data collected by the proposed device are explained in a single dataset. In the merged dataset, we combined the datasets generated by the proposed device and the smartphone PPG datasets [18,25] for the same purpose. This gave us some insights, which will be explained in due course.

4.3.1. Model building on a single dataset

Using the proposed device, a single dataset containing multiple trials of ppg signals from 50 subjects is generated. In Section 3.3.1, this dataset was discussed in greater detail. The proposed device acquired PPG signals that were largely free of high-frequency noise and baseline variations. The preprocessing techniques, which consisted of Gaussian filter denoising and ALS baseline corrections, remained unchanged across all trials. Even if baseline drift and high-frequency noise are present, the proposed signal processing model can collect a clean and acceptable PPG signal. This could ease the burden during data collection. On the preprocessed signal, numerous signal characteristics described in the methodology section were retrieved.

For training and testing purposes, eight models were developed on the single dataset. In Section 3.6, the models were analyzed. Using SEP in mmol/L, the performance of the models was evaluated, and the optimal model was determined.

Fig. 13 depicts the estimated Standard Error of Prediction (SEP) versus the number of principal components (PCs) obtained for PCR models constructed using different methods. The SEP was significantly greater for the PCR model built with the DelT features than for other methods. Error increased as the number of principal components increased, reaching 1.5 mmol/L at 11 PCs. For PCR models built with the first and second derivatives, a comparable change in SEP was observed. The model constructed with the first derivative had a

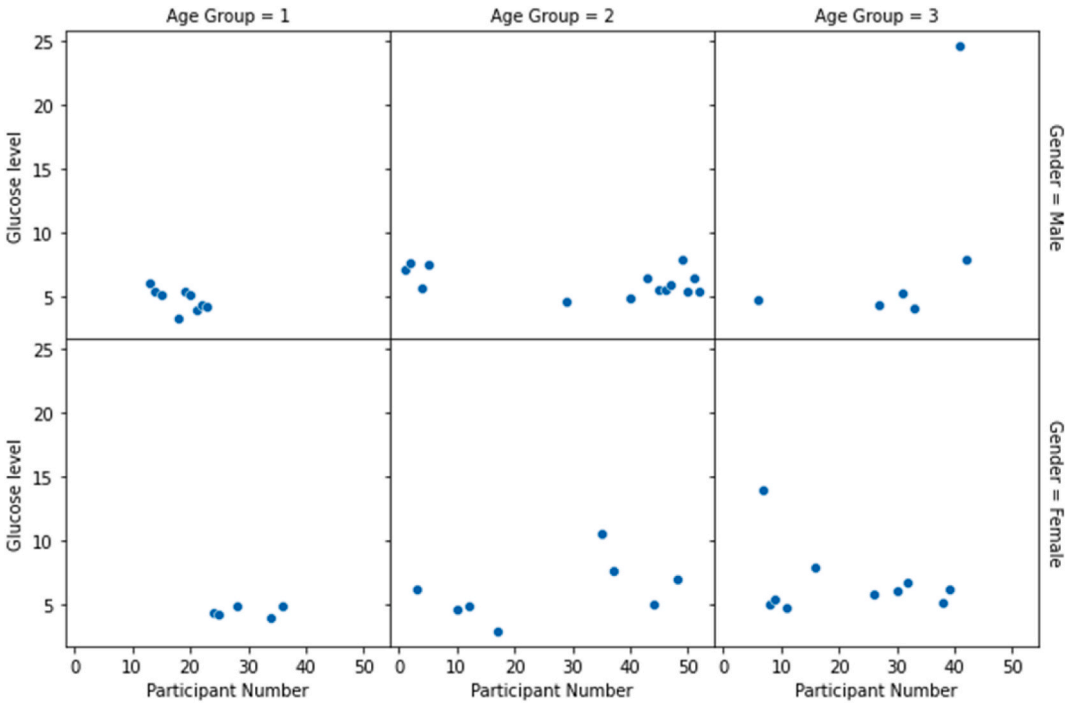

Fig. 12. Scatterplot of obtained data based on gender and age.

SEP of 0.9884 mmol/L for 2 PCs, which was slightly lower than the model constructed with the second derivative. In the model constructed with the 2nd Derivative Characteristic points, a significant decrease in SEP for all PCs could be observed. The lowest SEP achieved by this model with the first seven PCs was 0.7850 mmol/L, despite the fact that SEP in other PCs, such as PC = 4 to 6, is also within the acceptable range and significantly lower than the lowest SEP achieved by any model for any number of PCs.

Table 1 compares the performance of various PCR models in terms of the lowest SEP attained and the minimum number of PCs required. The raw signal's preprocessing and feature extraction significantly improved the PCR model's ability to predict outcomes. It is important to note, however, that systolic and diastolic features alone did not improve the accuracy, and that the performance of the signal's first and second derivatives was also unremarkable.

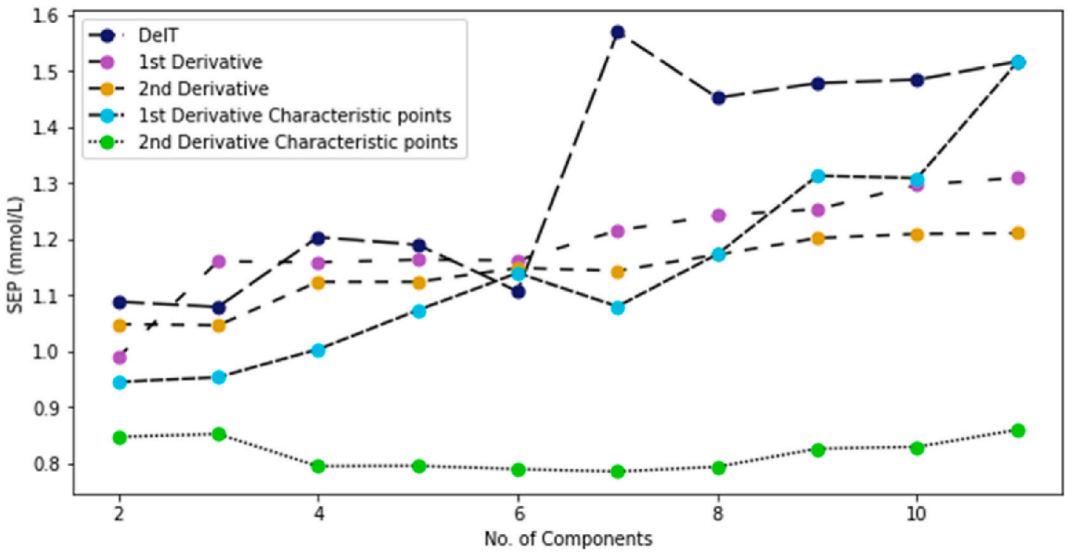

Fig. 13. Standard Error of Predictions (SEPs) against a different number of principal components (PCs) achieved for Principal Component Regression (PCR) model built with different preprocessing approaches using Dataset 1.

4.3.2. Model building on the merged dataset

The merged dataset is comprised of the dataset containing the PPG signal acquired by the proposed device as well as two additional datasets from our previous works [18,25]. One of these datasets contains ppg signals and the respective glucose levels of 52 subjects collected using a smartphone-based method in a prior study [18], while the other contains the same for 18 subjects. The smartphone sensors utilized in these two prior datasets vary as well. The combination of these datasets produced a total of 439 PPG signal trials. The same eight models were also built for training and testing on the merged dataset. Using SEP in mmol/L to evaluate the performance of the models.

Note that PPG trials collected through a smartphone are significantly noisier and more susceptible to motion interference. Even when obtained from the same subject, they exhibited considerable variation. In each of these trials, the quality of the PPG signals varied. The preprocessing techniques, which consisted of Gaussian filter denoising and ALS baseline corrections, remained unchanged across all trials. With the aid of the proposed signal processing model, an acceptable PPG signal can be collected despite baseline drift and high-frequency noise.

Estimated Standard Error of Prediction (SEP) versus Number of Principal Components (PCs) Obtained for PCR Models constructed using various methods is depicted in Fig. 14. The SEP values for various models were surprisingly close. Examining changes in SEP for various PCs reveals a similar trend for the majority of models, particularly those with first derivative, second derivative, and second derivative characteristic points. However, a significant SEP gap was observed between the model constructed with DelT features and the rest. The lowest SEP achieved by this model with the first nine PCs was 2.1835 mmol/L, and the SEPs for other PCs are significantly lower than the lowest SEP achieved by any model with any number of PCs.

For the remaining methods, a significant decrease in SEP was observed. Using a model constructed with the initial Derivative Characteristic points, the SEP was determined to be 2.2544 mmol/L with the initial ten PCs. In contrast, the lowest SEP was observed with eleven components in models that included first derivative and second derivative features at a concentration of 2.2590 mmol/L. When the PCR model was constructed with the DelT feature derived from signal preprocessing via Gaussian and ALS filtering with 9 PCs, the SEP was reduced even further to 2.1835 mmol/L. The feature extraction method significantly improved the predictive ability of the PCR model. Notably, systolic and diastolic features alone did not improve the accuracy, and the performance with second derivative features was also unremarkable. Table 2 compares the performance of different PCR models based on the lowest SEP attained and the minimum number of PCs required. Preprocessing and feature extraction on the raw signal had no effect on the predictive ability of the PCR model. It is crucial to note that the SEP based on the raw signal was lower than that of models with features, indicating that feature extraction did not improve accuracy.

4.4. Model integration on hardware

In section 3.4, we described a variety of models, and in section 4.3, we discussed the accuracy achieved by these models. The best model in terms of error rate and number of principal components has been incorporated into the hardware to complete the development of a fully portable, non-invasive device that can estimate glucose levels instantly. This device was then tested for two weeks on a subject. During this period, the subject was required to measure his or her glucose level daily before a meal (fasting) using both the proposed device and a commercially available invasive glucometer. The subject was instructed to adhere to a strict protocol. The subject was instructed to insert the index finger into the device, as shown in Fig. 15. When the user placed their finger comfortably, they pressed the start button. The device created a new data file on the SD card and displayed the recording progress of PPG data. In addition, an on-screen progress bar informed the participant of the duration of data collection. Once the progress bar reaches 100, a message indicating that PPG data has been successfully recorded is displayed. The subject was instructed to remove his or her finger and wait a few seconds while the hardware performed its calculations. After calculation, the predicted glucose reading is displayed in large font. The subject was required to manually record the date and glucose readings on a chart. In addition, we assisted the subject in measuring their blood glucose levels using a clinical glucometer Bioneme GM100 [26]. Bioneme GM100 results were also recorded in a manual chart to compare the proposed device's accuracy. Fig. 16 depicts that the difference between the predicted and actual results was small and within the acceptable range, and that our forecast was also accurate.

4.5. Building personalized model

With the current hardware and software models proposed, it is also possible to implement a completely user-centric, customized

Table 1
Comparison of performances of different PCR models.

Features	SEP (mmol/L)	Number of PCs
Xraw	1.0991	2
XrawAls	1.0018	3
XrawAlsGauss	0.9935	2
DelT	1.0784	3
1st Derivative	0.9884	2
2nd Derivative	1.0456	3
1st Derivative Characteristic points	0.9448	2
2nd Derivative Characteristic points	0.7850	7

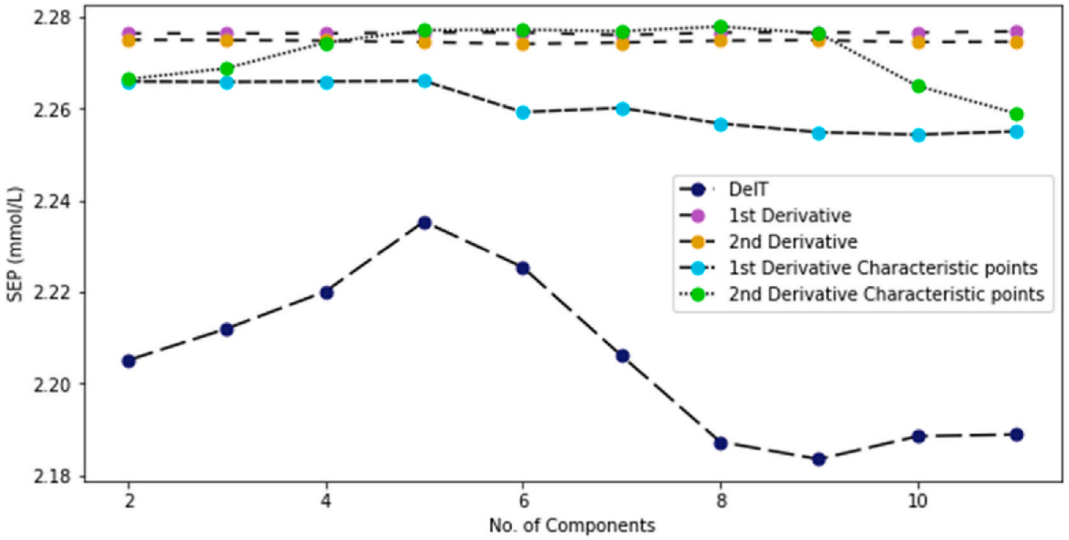

Fig. 14. Standard Error of Predictions (SEPs) against a different number of principal components (PCs) achieved for Principal Component Regression (PCR) model built with different preprocessing approaches using Dataset 3.

Table 2
Comparison of performances of different PCR models.

Features	SEP (mg/dL)	Number of PCs
Xraw	2.2847	8
XrawAls	2.2591	10
XrawAlsGauss	2.2763	10
DelT	2.1835	9
1st Derivative	2.2761	7
2nd Derivative	2.2742	6
1st Derivative Characteristic points	2.2544	10
2nd Derivative Characteristic points	2.2590	11

device. Fig. 17 provides a basic outline of such an implementation. In order to accomplish this, the user must upload his or her own PPG data and clinical glucose level to a cloud-based database for a predetermined amount of time. Note that our current GUI application is able to perform this task. The server will then regularly or at a predetermined interval train the model using newly received signals from the user. In other words, the model will be trained on the data of a specific user, and as a result, its accuracy is anticipated to be higher than that of a generic model. The model will then be downloaded to the device over the internet, which is currently accomplished by connecting the device to a computer via USB. This will make each of these devices intelligent and customized. Components such as PPG reading, GUI, a cloud-based database, and a server already exist in our proposed device. In addition, the ESP32 chip may enable Wi-Fi or Bluetooth connectivity.

5. Discussion

In this study, an entirely PCR-based model was developed. Based on our previous research [18,25], we found that the PCR and PLS models outperform others, such as the SVR and RFR models. The purpose of combining multiple datasets and conducting training on them was to determine if the ppg signal acquired via different acquisition tools could be combined for training purposes and if such model development would be advantageous. The lowest SEP achieved on a single dataset for seven PCs was 0.7850 mmol/L, which increased by a factor of three while being trained and tested on the merged dataset. Clearly, the model performed better after being trained on the dataset generated by the proposed device. However, we have already observed that smartphone PPG signal baseline drift and high-frequency noises vary significantly. Though, the signal processing model has made a big difference in the quality, but this may not be enough. Another point to note, the smartphone PPG were collected in the RGB spectrum as opposed to the infrared spectrum used by the proposed device. Consequently, the transmitted wavelength and signal quality may have contributed to a higher SEP for models constructed from the dataset generated by the proposed device.

Table 3 compares the techniques we used to determine how accurate we were with those in other works and provides a detailed look at other works in the same field. Here, we can observe how various studies have developed a variety of data collection techniques. Our approach to data collection is comparatively simple and offers users the greatest convenience. In addition, our model needed less duration of data than other models (1 min). We have the lowest error rate. Additionally, it takes the suggested devices about a minute

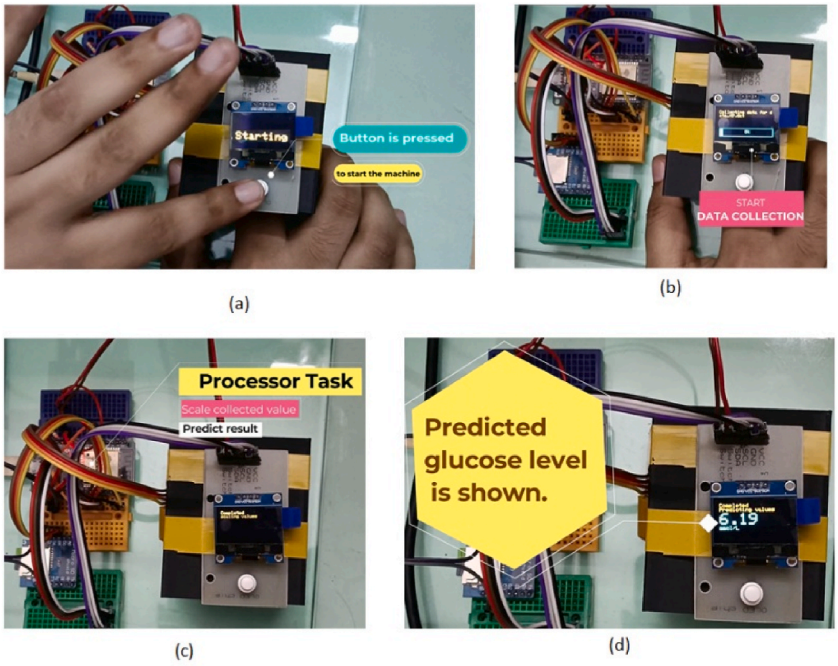

Fig. 15. Processes of checking glucose level using our proposed device; (a)Button is pressed to start taking readings, (b) PPG reading is collected from the user, and progress is displayed in real-time (c)Processor calculates the predicted glucose level. (d) The predicted glucose level is shown in a display with large font for greater accessibility.

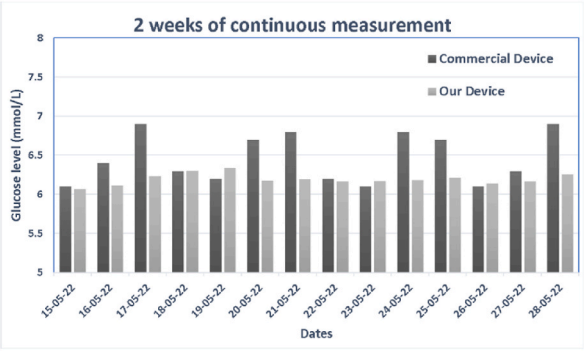

Fig. 16. Result after integration of model.

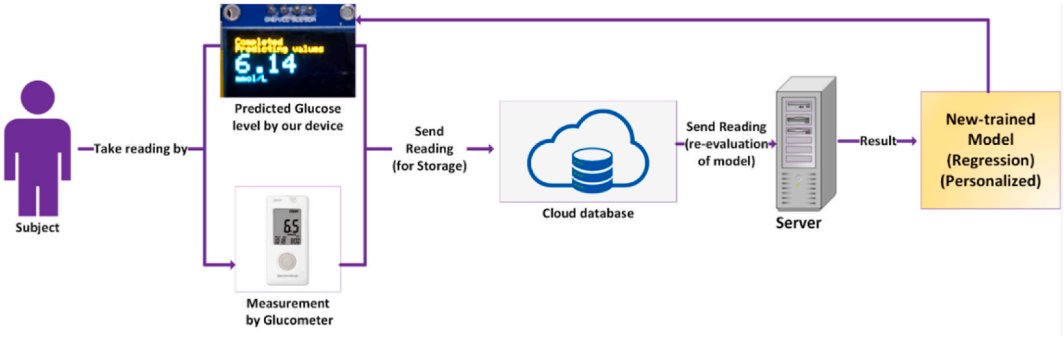

Fig. 17. Generation and setting of personalized model.

to predict glucose levels. The amount of time needed for detection was not specified by any of the methods before. We therefore have the quickest detection time based on the used method.

There are few human factors that can affect the system's performance. The enclosure of the proposed device restricts finger movement thus reducing motion interferences. In data modeling, gender and age variation have been taken into account. The model could be improved by incorporating more information on high glucose levels, on which we intend to work next. In addition, demographic information has not yet been incorporated into the study. In a future study, we might combine this information with signals to construct a model. Furthermore, the participants are from specific geographical regions. To our knowledge, this does not affect the PPG signal acquired. Glucose levels indicative of diabetes may, however, vary by region, according to some reports. With thorough analysis and testing, it will be possible to comment on this.

According to the ICs manufacturer's specifications, the device can operate effectively over a broad temperature range. Therefore, weather changes have no effect on performance. A recent report indicates, however, that seasonal variations may affect the average blood glucose level of diabetic patients. In the future, we may investigate this by collecting data and conducting experiments on the same group of participants during different seasons.

6. Conclusion

Here, we design, develop, and demonstrate a multipurpose intelligent medical device for the noninvasive measurement of blood glucose. The device is inexpensive and does not require consumables, such as strips, that incur recurring costs. It is portable and self-operating; a non-technical user can operate it without instruction. The user must place their fingertips on a sensor, and the result will appear on an integrated display immediately. A model deployed in the device's processor facilitates this estimation. The device can also serve as a valuable platform for the collection of PPG data for a variety of other applications. For this, we developed a graphical user interface (GUI) program that enables easier visualization of the collected data, saves it along with the labels, and automatically generates a dataset. We also demonstrated that the proposed device could be upgraded to a personalized, intelligent Internet of Things (IoT) medical device that learns the glucose levels of individuals to improve prediction. Planned additional experiments will implement what is depicted in Fig. 17. We believe that the proposed technique is significant because it provides a painless, inexpensive, and accurate method for monitoring glucose levels.

Author contribution statement

Tanzilur Rahman: Conceived and designed the experiments; Analyzed and interpreted the data.

Kazi Mosaddequr: Performed the experiments; Analyzed and interpreted the data; Contributed reagents, materials, analysis tools or data; Wrote the paper.

Data availability statement

Data will be made available on request.

Additional information

No additional information is available for this paper.

Declaration of competing interest

The authors declare that they have no known competing financial interests or personal relationships that could have appeared to influence the work reported in this paper.

Table 3
Performance comparison with existing works.

Reference	Number of Subjects	Data Duration	Mode of data collection	SEP value	RMSE	Portable prototype proposal	Time to detection
[15]	93	1 min	video	1.0172	–	No	–
[16]	26	4min SPO2	clinical PPG	5.56 to 8.33	–	Yes	–
[27]	93	5 min	Near-infrared spectroscopy	–	1.2194	Yes	–
[20]	–	30 min	Figer tip using CSSR sensor	–	–	Yes	–
[19]	111	15 s	fingertip video	–	1.461	No	–
[17]	51 samples	–	Human earlobe	–	0.099984	No	–
[21]	28	4 h	upper arm PPG	–	2.022	–	–
[18]	still ongoing	60 s	fingertip video by phone camera	0.9456	–	No	–
Proposed	110	1 min	fingertip by hardware	0.785	–	Yes	2 min

References

[1] P. Saeedi, et al., "Global and regional diabetes prevalence estimates for 2019 and projections for 2030 and 2045, in: ninth ed.Results from the International Diabetes Federation Diabetes Atlas, vol. 157, Diabetes Research and Clinical Practice, Sep. 2019, 107843 https://doi.org/10.1016/j.diabres.2019.107843, 157.

[2] Monika Klimek-Tulwin, Joanna Knap, Mateusz Reda, Marta Masternak, History of glucose monitoring: past, present, future, J Edu, Health Sport 9 (2019) 222–227, https://doi.org/10.5281/zenodo.3397600.

[3] T. Shang, J.Y. Zhang, A. Thomas, et al., Products for monitoring glucose levels in the human body with non -invasive optical, non-invasive fluid sampling, or minimally invasive technologies, J. Diabetes Sci. Technol. 16 (1) (2022 Jan) 168–214, https://doi.org/10.1177/19322968211007212.PMID, 34120487; PMCID: PMC8721558.

[4] Cai A, Gutow H, Mahoney K, et al. CGM 4Q20 industry roundup – record CGM sales of $1.6 billion, rising 26% YOY – March 9, 2021. Close Concerns Knowledgebase. March 9, 2021. Accessed March 15, 2021 https://www.closeconcerns. com/knowledgebase/r/be9b1ac7.

[5] S. Cousins, N.S. Blencowe, J.M. Blazeby, What is an invasive procedure? A definition to inform study design, evidence synthesis and research tracking, BMJ Open 9 (7) (2019), e028576, https://doi.org/10.1136/bmjopen-2018-028576.

[6] W. Villena Gonzales, A.T. Mobashsher, A. Abbosh, The progress of glucose monitoring—a review of invasive to minimally and non-invasive techniques, devices and sensors, Sensors 19 (4) (2019) 800, https://doi.org/10.3390/s19040800.

[7] D.C. Klonoff, J.F. Perz, Assisted monitoring of blood glucose: special safety needs for a new paradigm in testing glucose, J. Diabetes Sci. Technol. 4 (5) (2010) 1027–1031, https://doi.org/10.1177/193229681000400501.

[8] H.-C. Wang, A.-R. Lee, Recent developments in blood glucose sensors, J. Food Drug Anal. 23 (2) (2015) 191–200, https://doi.org/10.1016/j.jfda.2014.12.001.

[9] J.A. Tamada, S. Garg, L. Jovanovic, K.R. Pitzer, S. Fermi, R.O. Potts, Non -invasive glucose monitoring: comprehensive clinical results. Cygnus Research Team, JAMA 282 (19) (1999) 1839–1844, https://doi.org/10.1001/jama.282.19.1839.

[10] Nemaura Medical, Nemaura medical. https://nemauramedical.com/29. (Accessed 14 December 2020).

[11] H.M. Heise, S. Delbeck, R. Marbach, Non -invasive monitoring of glucose using near-infrared reflection spectroscopy of skin— constraints and effective novel strategy in multivariate calibration, Biosensors 11 (3) (2021) 64, https://doi.org/10.3390/bios11030064.

[12] C. Jurysta, N. Bulur, B. Oguzhan, et al., Salivary glucose concentration and excretion in normal and diabetic subjects, J. Biomed. Biotechnol. 2009 (2009), 430426, https://doi.org/10.1155/2009/430426.

[13] W.F. March, A. Mueller, P. Herbrechtsmeier, Clinical trial of a non -invasive contact lens glucose sensor, Diabetes Technol Ther 6 (6) (2004) 782–789, https://doi.org/10.1089/dia.2004.6.782.

[14] M.-S.-M. Soares, M.-M.-V. Batista-Filho, M.-J. Pimentel, I.-A. Passos, E. Chimenos-Kustner, Determination of salivary glucose in healthy adults, Med. Oral, Patol. Oral Cirugía Bucal 14 (10) (2009) e510–e513, https://doi.org/10.4317/medoral.14.e510.

[15] M.R. Haque, S.M.T.U. Raju, M.A.-U. Golap, M.M.A. Hashem, in: " A Novel Technique for Non-invasive Measurement of Human Blood Component Levels from Fingertip Video Using DNN Based Models,", vol. 9, IEEE Access, 2021, pp. 19025–19042, https://doi.org/10.1109/ACCESS.2021.3054236. https://ieeexplore.ieee.org/abstract/document/9335002.

[16] S.S. Gupta, T.H. Kwon, S. Hossain, K.D. Kim, Towards non-invasive blood glucose measurement using machine learning: an all-purpose PPG system design, Biomed. Signal Process Control 68 (2021), 102706. https://www.sciencedirect.com/science/article/abs/pii/S1746809421003037.

[17] Q. Li, X. Xiao, T. Kikkawa, Non -invasive blood glucose level detection based on matrix pencil method and artificial neural network, J. Electr. Eng. Technol. 16 (2021) 2183–2190, https://doi.org/10.1007/s42835-021-00719-3.

[18] T.T. Islam, M.S. Ahmed, M. Hassanuzzaman, S.A. Bin Amir, T. Rahman, Blood glucose level regression for smartphone PPG signals using machine learning, Appl. Sci. 11 (2) (Jan. 2021) 618, https://doi.org/10.3390/app11020618.

[19] M.A.U. Golap, S.T.U. Raju, M.R. Haque, M.M.A. Hashem, Hemoglobin and glucose level estimation from PPG characteristics features of fingertip video using MGGP-based model, Biomed. Signal Process Control 67 (2021), 102478. https://www.sciencedirect.com/science/article/abs/pii/S1746809421000756.

[20] A.E. Omer, G. Shaker, S. Safavi-Naeini, et al., Low-cost portable microwave sensor for non-invasive monitoring of blood glucose level: novel design utilizing a four-cell CSRR hexagonal configuration, Sci. Rep. 10 (2020), 15200, https://doi.org/10.1038/s41598-020-72114-3.

[21] M. Mueller, M.S. Talary, L. Falco, O. De Feo, W.A. Stahel, A. Caduff, Data processing for non-invasive continuous glucose monitoring with a multisensor device, J. Diabetes Sci. Technol. 5 (3) (May 2011) 694–702, https://doi.org/10.1177/193229681100500324.

[22] "OPT101," Ti.com. https://www.ti.com/product/OPT101, 2015.

[23] J. Peng, S. Peng, A. Jiang, J. Wei, C. Li, J. Tan, Asymmetric least squares for multiple spectra baseline correction, Anal. Chim. Acta 683 (1) (Dec. 2010) 63–68, https://doi.org/10.1016/j.aca.2010.0.

[24] S.W. Smith, Digital Signal Processing: A Practical Guide for Engineers and Scientists, Elsevier, Amsterdam, The Netherlands, 2013.

[25] T.T. Chowdhury, T. Mishma, S. Osman, T. Rahman, Estimation of blood glucose level of type-2 diabetes patients using smartphone video through PCA-DA, ", Proceedings of the 6th International Conference on Networking, Systems and Security - NSysS '19 (2019) https://doi.org/10.1145/3362966.3362983.

[26] "Rightest GM100 glucometer," bionime.com. https://www.bionime.com/GM100.html (Accessed November. 9, 2022).

[27] P. Jain, A.M. Joshi, S.P. Mohanty, in: " iGLU: an Intelligent Device for Accurate Noninvasive Blood Glucose-Level Monitoring in Smart Healthcare,", vol. 9, IEEE Consumer Electronics Magazine, 2020, pp. 35–42, https://doi.org/10.1109/MCE.2019.2940855, 1.